

The complexity of narrowband echo envelopes as a function of fish side-aspect angle

Debby L. Burwen, Patrick A. Neelson, Steven J. Fleischman, Timothy J. Mulligan, and John K. Horne

Burwen, D. L., Neelson, P. A., Fleischman, S. J., Mulligan, T. J., and Horne, J. K. 2007. The complexity of narrowband echo envelopes as a function of fish side-aspect angle. – *ICES Journal of Marine Science*, 64: 1066–1074.

High-frequency, narrowband acoustic signals may contain more information on fish size and orientation than previously thought. Our observations of dual frequency identification sonar (DIDSON) images of fish orientation paired with split-beam echo envelopes helped clarify why metrics such as echo duration have performed better than target strength measurements when predicting salmon lengths at side aspect. Fish orientation has a pronounced effect on the duration and shape of split-beam echo envelopes from large (80–130 cm) salmon insonified at side aspect. At near-normal aspect angles, echo envelopes are unimodal, symmetrical, and resemble echo envelopes from calibration spheres. With increasing oblique-aspect angle, echo shapes become less symmetrical as the number of peaks increases, and echo duration and amplitude become more variable. Using angle and range coordinates, peaks in an echo envelope can be traced to their origin on a DIDSON image. At oblique-aspect angles, discrete peaks develop that are reflected from regions close to the head and tail. In addition, the distance between peaks increases with increasing aspect angle and is larger than can be explained by swimbladder length.

Keywords: aspect angle, DIDSON sonar, echo duration, side aspect, species classification, split-beam echosounder, target strength.

Received 19 September 2006; accepted 25 April 2007; advance access publication 12 June 2007.

D. L. Burwen and S. J. Fleischman: Alaska Department of Fish and Game, 333 Raspberry Road, Anchorage, AK 99518, USA. P. A. Neelson and J. K. Horne: School of Aquatic and Fishery Sciences, University of Washington, PO Box 355020, Seattle, WA 98195, USA. T. J. Mulligan: Pacific Biological Station, Nanaimo, British Columbia, Canada V9T 6N7. Correspondence to D. L. Burwen: tel: +1 907 267 2225; fax: +1 907 267 2401; E-mail: debby_burwen@fishgame.state.ak.us

Introduction

Variability in echo-intensity metrics such as target strength (TS) often constrains our ability to discriminate among fish species. Unique conditions associated with side-looking (i.e. horizontally aimed) sonar applications exacerbate difficulties when discriminating species on the basis of acoustic size. Fish are insonified from the side, where swimming behaviour causes more variability in aspect and body curvature, resulting in greater variability in TS. Fish are often large relative to the acoustic wavelength and beam diameter, because they are insonified at short ranges (Dawson *et al.*, 2000). Further, signal-to-noise ratios are often low because of interference from acoustic boundaries (surface and bottom), which can lead to bias in split-beam estimates of position (Kieser *et al.*, 2000; Mulligan, 2000) and TS (Fleischman and Burwen, 2000). A typical result in side-looking applications is that mean backscattering cross section can differ by 10 decibel (dB) or more for two fish of the same species and identical length (Fleischman and Burwen, 2000). Consequently, using TS to discriminate between species can be difficult, if not impossible, even when species differ substantially in length. In side-looking riverine applications, we found that echo duration (i.e. the width of an echo measured at the half-power point), and variability of echo duration, are better predictors of fish length than are TS measurements (Burwen and Fleischman, 1998; Burwen *et al.*, 2003). However, the mechanisms responsible for the relationship

observed between echo duration and fish length have not been explained.

Recent investigations synchronizing a split-beam echosounder with a high-resolution multibeam sonar provided insights into why echo length and its variability outperform TS as a predictor of fish length at side aspect. The dual frequency identification sonar (DIDSON, Belcher *et al.*, 2001; see <http://soundmetrics.com/>) produces high-resolution images of fish at ranges up to 15 m (Burwen *et al.*, in press). It uses an acoustic lens system and multiple transmissions to produce composite images approaching video quality. By aligning the DIDSON and split-beam acoustic axes and synchronizing the transmissions, we were able to observe the effects of fish behaviour, as displayed by the DIDSON, on the corresponding split-beam echo envelopes from both tethered and free-swimming chinook (*Oncorhynchus tshawytscha*) salmon.

Here, we examine paired echoes from the two acoustic systems to investigate how complex echo-envelope shapes are influenced by fish orientation (i.e. aspect angle and swimming motion), length, and transmitted pulse length. It is well documented that echo amplitude and TS are highly influenced by fish orientation in both dorsal (Foote, 1980a; MacLennan *et al.*, 1990) and side (Love, 1969; Dahl and Mathisen, 1983; Kubecka, 1994; Lilja *et al.*, 2004) aspect. Those studies, though, did not examine corresponding changes in the duration or shape of the echo envelope

associated with changes in fish orientation. We show that relatively minor changes in fish aspect angle can produce elongated and even multi-peaked echo shapes. We also provide evidence that modes in the echo envelope (or separate peaks) can be associated with specific scattering surfaces along the fish body. Finally, we show how information related to the size and the orientation of the fish can be extracted from echo envelopes using a simple geometric model.

Material and methods

Echoes from salmon were collected using a split-beam echosounder synchronized with a multibeam sonar during July 2002 and August 2005 at an acoustic monitoring site located 14 km (8.5 miles) from the mouth of the Kenai River, Alaska (for site details, see Miller and Burwen, 2002). The 100-m wide river is tidally influenced, with water depth at mid-channel varying from 3 to 8 m. Water temperatures ranged from 10 to 15°C. The mud bottom provides a low backscatter surface when the beam is aimed along the river bottom. A gradual and uniform bottom slope allows a large proportion of the water column to be insonified without excessive noise and acoustic shadowing effects.

Chinook salmon were captured with gillnets and held in live pens or totes until they were individually tethered for TS and orientation measurements. To isolate the fish from other targets, a cable tie was inserted through a small hole punched in the lower jaw and then attached to ~10 m of Dacron fishing line that led to a 2.8 kg weight (Figure 1). A second 6-m section of Dacron line connected the weight to a buoy on the surface. The buoy was attached with polypropylene line to an upstream anchor. River flow and average fish orientation were approximately normal to the acoustic axes, with ranges to targets varying between 3 and 15 m. Total length (tip of nose to fork of tail), body width, and body depth of each fish were measured prior to tethering.

The multibeam sonar and split-beam transducer were mounted on a remote-controlled, dual-axis rotator to allow precise aiming. The acoustic axes of the split-beam and multibeam transducers were vertically aligned and directed across the river perpendicular to the river flow. The beams were then aimed to insonify the near-bottom region of the river, because this area was preferred by both tethered and free-swimming salmon.

The DIDSON multibeam sonar uses a 96-element transducer array to generate a 14° vertical by 29° horizontal beam with a 0.3° horizontal resolution. Each image or frame consists of eight

consecutive pings and is acquired in 0.150 s (i.e. 0.018 s ping⁻¹). In high-frequency mode, the DIDSON's image is sequentially built from eight sets of 12 beams fired simultaneously (Belcher *et al.*, 2001; Sound Metrics Corporation, 2004). The use of composite images reduces cross-talk among beams, but the process may allow fish movement during the frame-composition cycle. Transmit pulse duration was set at 0.032 ms, and frame rates varied from 4 to 8 frames s⁻¹ in 2002 and fixed at 6 frames s⁻¹ in 2005. The DIDSON multibeam sonar triggered the split-beam echosounder 0.02 s before the start of each frame to provide near-synchronous samples from both instruments. Approximately 0.15 s was required to build each DIDSON frame, resulting in a cumulative delay of 0.17 s following each split-beam transmission.

Split-beam data were collected using a 200 kHz Model 241 (Hydroacoustics Technology, Inc.) echosounder and a 2.9° by 10° vertical by horizontal beam transducer with a nearfield of 3.1 m. The transmission rate similarly varied between 4 and 8 pings s⁻¹ in 2002 and was fixed at 6 pings s⁻¹ in 2005. Most data were collected using a fixed transmitted pulse duration of 0.2 ms. Limited data were also acquired using the fast multiplexing capability of the echosounder to sample alternately at 0.2 and 0.4 ms or between 0.1, 0.2, and 0.3 ms. Split-beam echo returns were collected using a -42 dB noise threshold. User-selected, single-echo detection criteria (echo-duration filters) were not applied, but the echosounder signal-processing logic limited recorded echo duration to twice that of the broadcast pulse duration, as measured at the half-power points. Echo range and phase measures at peak amplitude were based on the echosounder-processed data (i.e. single-target detections), where signal returns were digitally sampled at 48 kHz. This relatively high sampling rate provided measurements spaced ~1/64 m apart along the envelope (assuming *c*, the speed of sound, is 1500 m s⁻¹). The unprocessed digital samples used to describe echo-envelope shapes were output at a lower 12 kHz digitization rate (~1/16 m apart at *c* = 1500 m s⁻¹).

Images from the DIDSON frames were matched to echo-envelope data from the split-beam echosounder. Common events such as the passage of a free-swimming fish at a specific time and range were used to corroborate the synchronization of the two data files. Because the DIDSON frames and the split-beam system display data had the same two-dimensional coordinates (horizontal angle and range), it was possible to match split-beam echo peak(s) to their origin on the surface of the fish in the DIDSON image. Using software tools, the aspect angle of a fish was measured from the DIDSON images by taking the deviation from perpendicular of a line drawn through the lengthwise axis of the fish from the tip of the snout to the tip of the tail (Figure 2).

When split-beam echo envelopes contained two peaks that were detected as single targets, it was possible to estimate fish length (\hat{L}) using the difference in time of arrival between peaks (see also Ehrenberg and Johnston, 1996; Stanton *et al.*, 2003) and the aspect angle of the fish (Figure 3):

$$\hat{L} = \frac{D}{\sin \theta}, \quad (1)$$

where *D* is the distance between peaks (in cm) ($D = \Delta t c / 2$), Δt the time separation between peaks, *c* the speed of sound (1457 m s⁻¹), and θ is the angle between the incident sound wave and the lengthwise axis of the fish (i.e. aspect) in the lateral plane (see Figure 2).

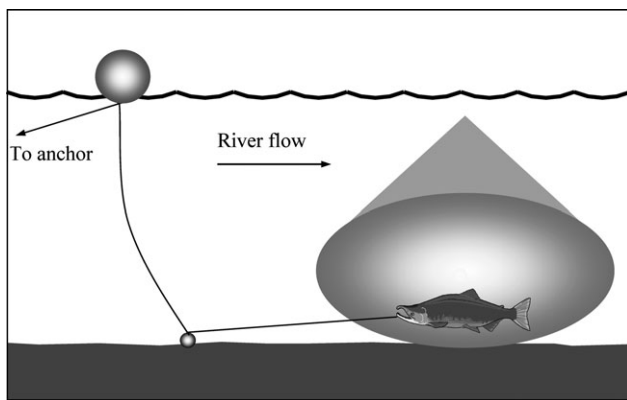


Figure 1. The tethering system used to position fish in side-looking sonar beams.

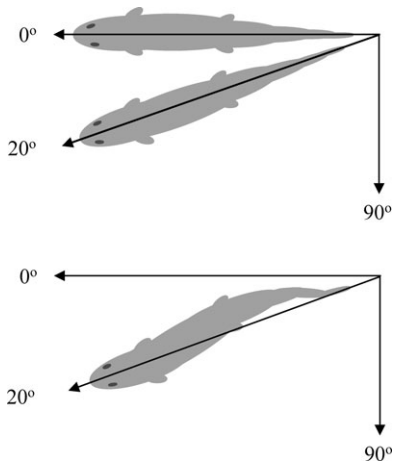


Figure 2. Coordinate system used to define side-aspect angle (θ). Aspect angle was measured from the DIDSON images by taking the deviation from the perpendicular of a line drawn through the lengthwise axis of the fish from the tip of the snout to the tip of the tail when the body was relatively straight (top) or curved (bottom). At an aspect angle normal to the incident sound wave, $\theta = 0^\circ$. Head-on aspect occurs at $\theta = 90^\circ$.

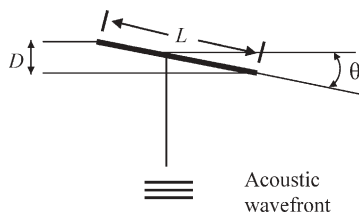


Figure 3. Geometry to predict fish length (L) from the difference in time of arrival between the resolved echo-envelope peaks and the aspect angle of the fish (see also Ehrenberg and Johnston, 1996).

Results

Echo envelopes varied in duration, intensity, and in the number of peaks as fish orientations deviated from the normal aspect. As a baseline, a 38.1 mm, tungsten carbide, calibration sphere returned a unimodal echo envelope consistent with the expected shape, duration, and intensity of a point-source target (Figure 4). Figure 5 shows a sequence of echo envelopes paired with DIDSON images returned from a tethered, 108 cm chinook salmon, where the aspect angle increased from 0 to 25°. The transmitted pulse length used in this sequence was 0.2 ms. At normal incidence (Figure 5a), the echo envelope is unimodal and resembles the echo envelope of the standard target (Figure 4). When the fish is orientated 15° from normal (Figure 5b), the echo envelope develops three distinct peaks, with each peak less than half the amplitude of the echo from the fish at normal aspect (Figure 5a). At 20 and 25° from normal (Figure 5c and d), two distinct echoes were returned. Similar echo-envelope shapes were returned from free-swimming fish. For example, in a series of paired echo envelopes and DIDSON images of a free-swimming chinook salmon migrating upstream (Figure 6), elongated and multi-peaked split-beam echoes were observed as the orientation and curvature of the fish varied. The first three panels (Figure 6a–c) show multi-peaked echo envelopes when the fish enters the insonified volume at oblique-aspect angles. The remaining panels (Figure 6d–l) illustrate changes in body curvature and echo-envelope shapes through two tail-beat cycles as the fish continues to swim upstream. Multi-peaked (Figure 6 h, j, and l) and elongated or asymmetrical single-peaked echoes (Figure 6d and k) are present when aspect angles deviate from normal.

The transmitted pulse length affected the occurrence of multi-peaked echoes. In Figure 7, three echograms display data collected from the same tethered chinook salmon shown in Figure 5 using fast multiplexed (alternating), transmit pulse widths of 0.1 (Figure 7a), 0.2 (Figure 7b), and 0.3 ms (Figure 7c). At 0.1 ms,

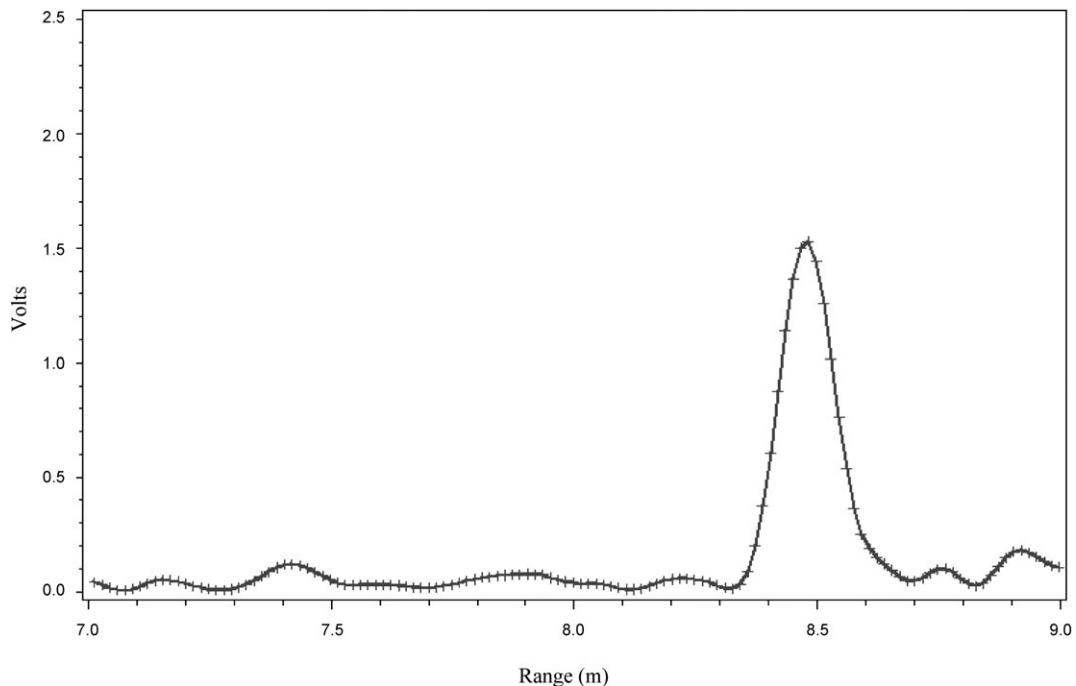


Figure 4. Echo envelope returned from a 38.1-mm diameter, tungsten carbide sphere insonified at 200 kHz with a 0.2 ms pulse.

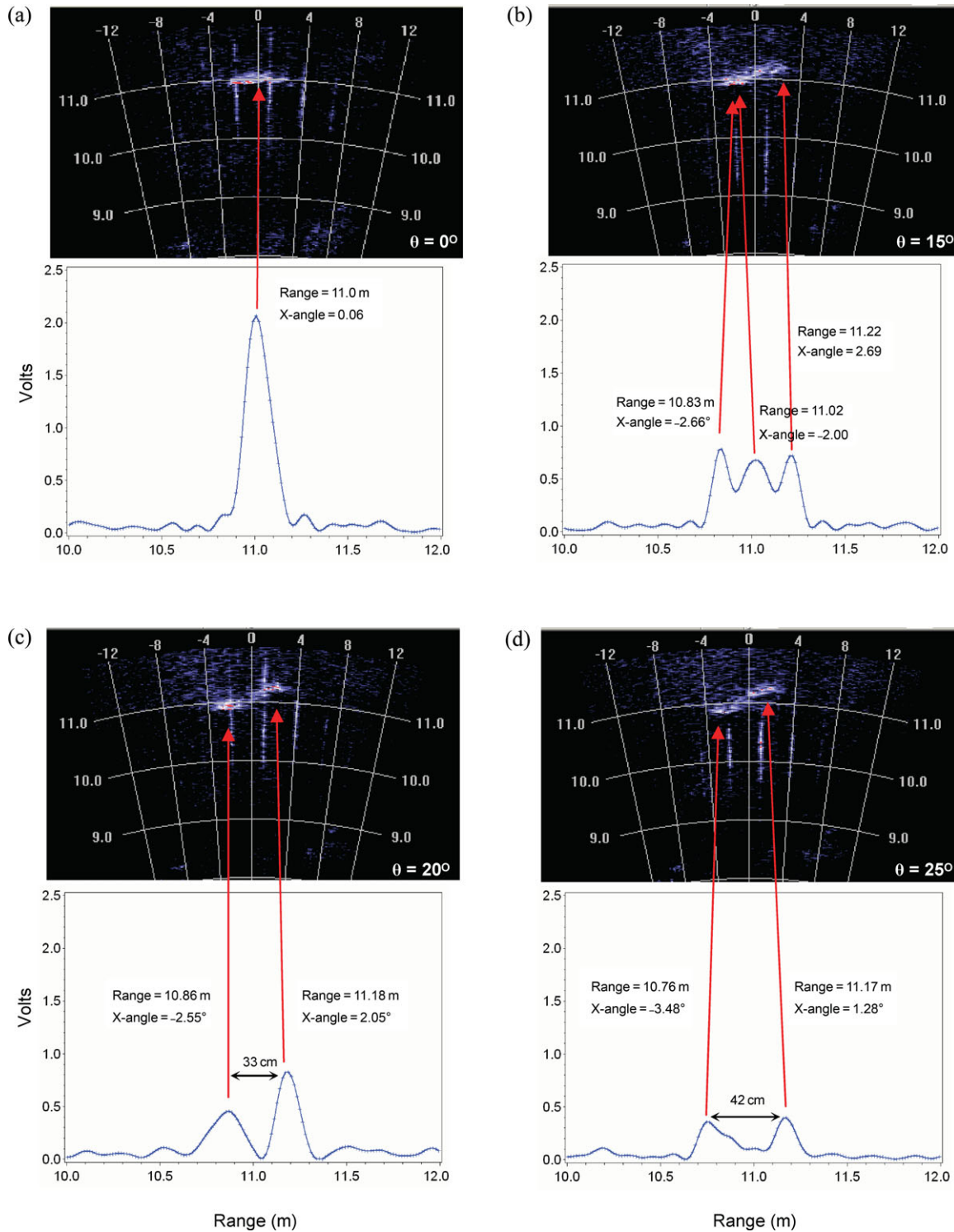


Figure 5. DIDSON images and the corresponding echo envelopes from a tethered, 108 cm chinook salmon at four side-aspect angles: (a) 0, (b) 15, (c) 20, and (d) at 25°. The fish is swimming against the current from right to left. The coordinates for range and horizontal split-beam angle (X-angle) of the echo peaks are given. The arrows map the split-beam echo-envelope peaks to the DIDSON image. The echo peaks generally correspond to high backscatter areas (red pixels) on the DIDSON image.

the range resolution is 7.3 cm, and the white arrows mark 14 occurrences of two single-target detections being received from the same fish with a single transmitted pulse. The number of multiple detections decreases to eight occurrences at 0.2 ms (range

resolution 14.5 cm), and to just four occurrences at 0.3 ms (range resolution 21.9 cm). Figure 8 shows the influence of the transmitted pulse length on the shape of the echo envelope. Echo envelopes from Figure 5 generated by a 0.2 ms transmitted

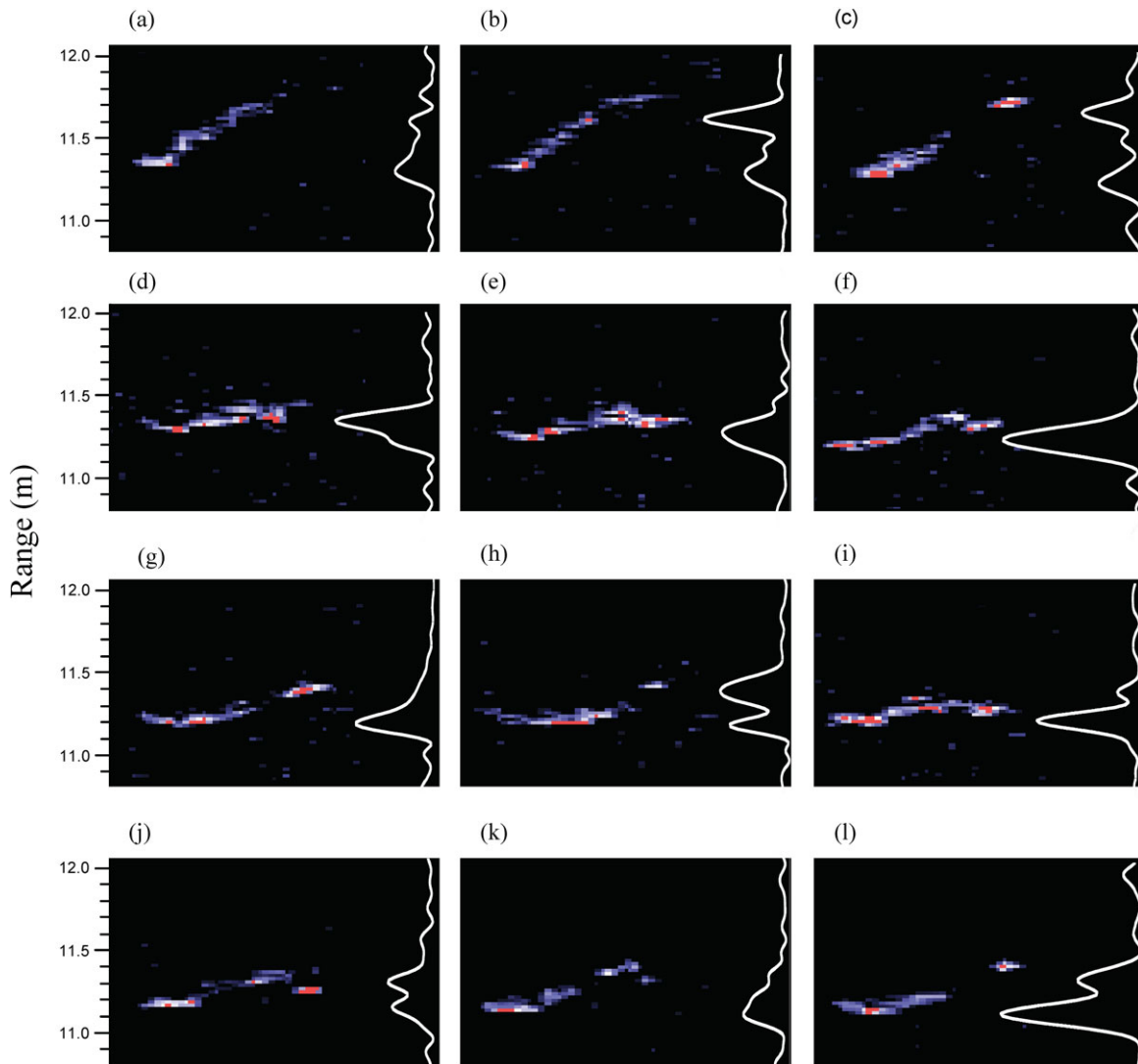


Figure 6. DIDSON images and the corresponding echo envelopes of a chinook salmon as it swims upstream through the sonar beams (from right to left). The range axis applies to the DIDSON image and the split-beam echo trace. Panels (a), (b), and (c) show the fish at high side-aspect angles as it first enters the beams. Panels (d)–(l) depict two full tail-beat cycles.

pulse are paired with those generated by a 0.4 ms pulse through fast multiplexing. Despite the short delay between the two pulses, the effect of the longer pulse on the echo shape is apparent. Echoes from the longer transmitted pulse length have a smoother appearance and the distinct multiple peaks observed at 0.2 ms have been lost at 0.4 ms (Figure 8b and d).

Comparison of synchronized data from the split-beam echosounder and the multi-beam sonar provide compelling evidence that complex echo envelopes result from reflections originating from multiple parts of the fish body, including the head and the tail. Echo-envelope peaks in Figure 5 could be mapped to their origins on the fish body shown on the DIDSON image using their common angle and range coordinates (red arrows). Using coordinates from the sample data, the first, second, and third peaks shown in Figure 5b originated from the head, body, and tail regions of the fish. At 20° and 25° off normal (Figure 5c and d), two echoes that met single-target detection criteria were returned from a single transmitted pulse. Coordinates of the

split-beam, single-target detection peaks indicate that the first peak originated from the head and the second from the tail.

When a fish is relatively straight and at highly oblique-aspect angles (e.g. Figure 5c and d), the aspect angle from the DIDSON frame and the range separation of the split-beam, single-echo detection peaks can be used to estimate fish length [Equation (1), Figure 3]. The series of frames and echoes in Figure 5 demonstrates that as aspect angle varies from normal incidence, multiple peaks appear (Figure 5b) and the original peak may even separate into two peaks that meet single-target detection criteria (Figure 5c and d). The distance between the first and the second peaks depends on the orientation angle (Figure 3). As the aspect angle increased from 20° (Figure 5c) to 25° (Figure 5d), the distance between echo peaks increased from 33 to 42 cm. This increase in echo peak separation is consistent with the increased separation between the anterior and posterior backscattering surfaces that was evident at steeper aspect angles. Using Equation (1), estimated lengths of this 108 cm fish are 96 cm in Figure 5c ($\theta = 20^\circ$); 33 cm

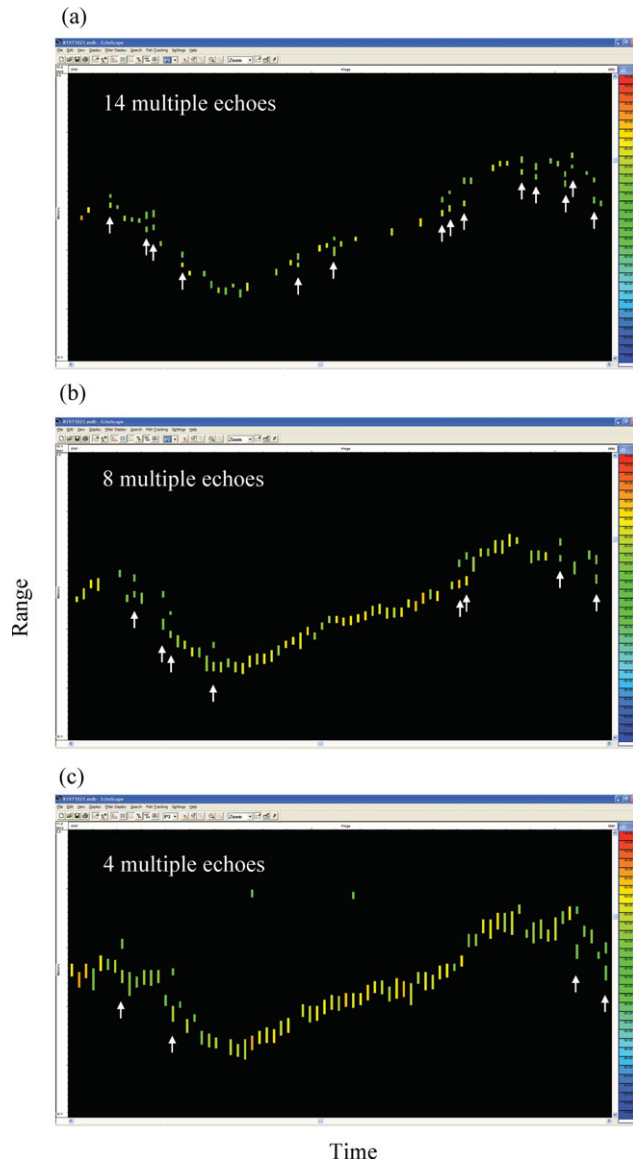


Figure 7. Split-beam echograms showing a tethered chinook salmon 108 cm long insonified at: (a) 0.1, (b) 0.2, and (c) 0.3 ms. Occurrences of multiple returns from the fish are indicated by white arrows. Each echogram displays 5 m in range and 222 pings (10 pings s^{-1}).

peak separation) and 99 cm in Figure 5d ($\theta = 25^\circ$; 42 cm peak separation).

Discussion and conclusions

Our results indicate that the shape of the echo envelope from large salmonids at 200 kHz is influenced by target orientation, target length, and transmitted pulse length. Target orientation includes aspect angle and the shape or the curvature of the fish, i.e. whether straight, convex, concave, or s-shaped. Echo envelopes were modified with only modest changes in aspect angle. Envelope shapes shown in Figure 5 are representative of those observed for large (80–130 cm), tethered chinook salmon. As the aspect angle of the fish increased, echo amplitude decreased, and echo duration increased. These elongated echo envelopes

often developed multiple peaks similar to Figure 5b, but typically only one was accepted as a single target. For example, the first peak in Figure 5b was accepted by the echosounder as a single target, but the other two peaks were ignored or excluded. At more oblique-aspect angles (Figure 5c and d), discrete backscatter regions of the fish produced two individual echoes that met single-target detection criteria, i.e. two single-target detections from the same fish from a single transmitted pulse. This process in which one elongated echo separates into two echoes of shorter duration is evident when the scattering surface of the fish, through a combination of body curvature and aspect angle, exceeds the range resolution of the echosounder ($c\tau/2$, in this case 14.6 cm). The variation in echo duration introduced may help explain why echo duration variability has shown an even stronger correlation with fish length than mean echo duration (Burwen and Fleischman, 1998; Burwen *et al.*, 2003). It seems reasonable to expect that for a given transmitted pulse length, longer fish will require smaller changes in aspect angle to exceed the range resolution of the echosounder. It also follows that the shorter the transmitted pulse length, the smaller will be the aspect angle or length required to modify the envelope shape (Figures 7 and 8).

When fish are insonified in dorsal aspect, conventional thinking is that most energy will be reflected from the swimbladder, when present (Harden-Jones and Pearce, 1950; Foote, 1980b). However, pairing of DIDSON images with split-beam echo envelopes illustrates that, depending on target orientation, other anatomical structures can contribute to target backscatter and can influence the shape of the resulting echo. Several lines of evidence support the assertion that scattering features along the fish body are not confined to the swimbladder (see also Nash *et al.*, 1987). First, range and angle information used to match echo-envelope peaks to their origin on the fish indicate that the peaks originated closer to the head and tail than would be expected if all energy was reflected from the swimbladder. Second, estimates of fish length based on echo peak separations and aspect angles in Figure 5c and d corresponded to 89 and 92% of the actual fish length. In similar calculations, Stanton *et al.* (2003) found that use of 90–95% of the actual fish length (i.e. effective acoustic length) resulted in the best estimate of separation time [i.e. $\Delta\tau$ in Equation (1)] between the first and second peak in echo envelopes. Finally, in an experiment where the DIDSON and split-beam transducer axes were centred first on the body and then on the tail of a large (1180 mm) chinook salmon, we found that well-defined echoes were returned consistently from the tail region (Figure 9). The split-beam angle and range coordinates indicated that the echo peaks originated from the tail of the fish (Figure 9c). Moreover, these echoes appeared more variable in range and duration than those collected from the same fish where the transducer was centred on the body midsection (Figure 9a and b).

Contributions from non-gas-filled anatomical structures to multi-peaked echoes have been observed for other fish species. A transition from single to multi-peaked echoes was observed by Stanton *et al.* (2003) as alewife (*Alosa pseudoharengus*) were rotated from normal incidence in both the dorsal or ventral and lateral planes. Stanton *et al.* (2003) proposed that peaks originated from individual scattering features along the length of the fish body that were separated by more than the range resolution of 2 cm. Sun *et al.* (1985) provided supporting evidence through the matching of peaks in echo envelopes to the skull, spinal column, and swimbladder of yellow perch (*Perca flavescens*). Our

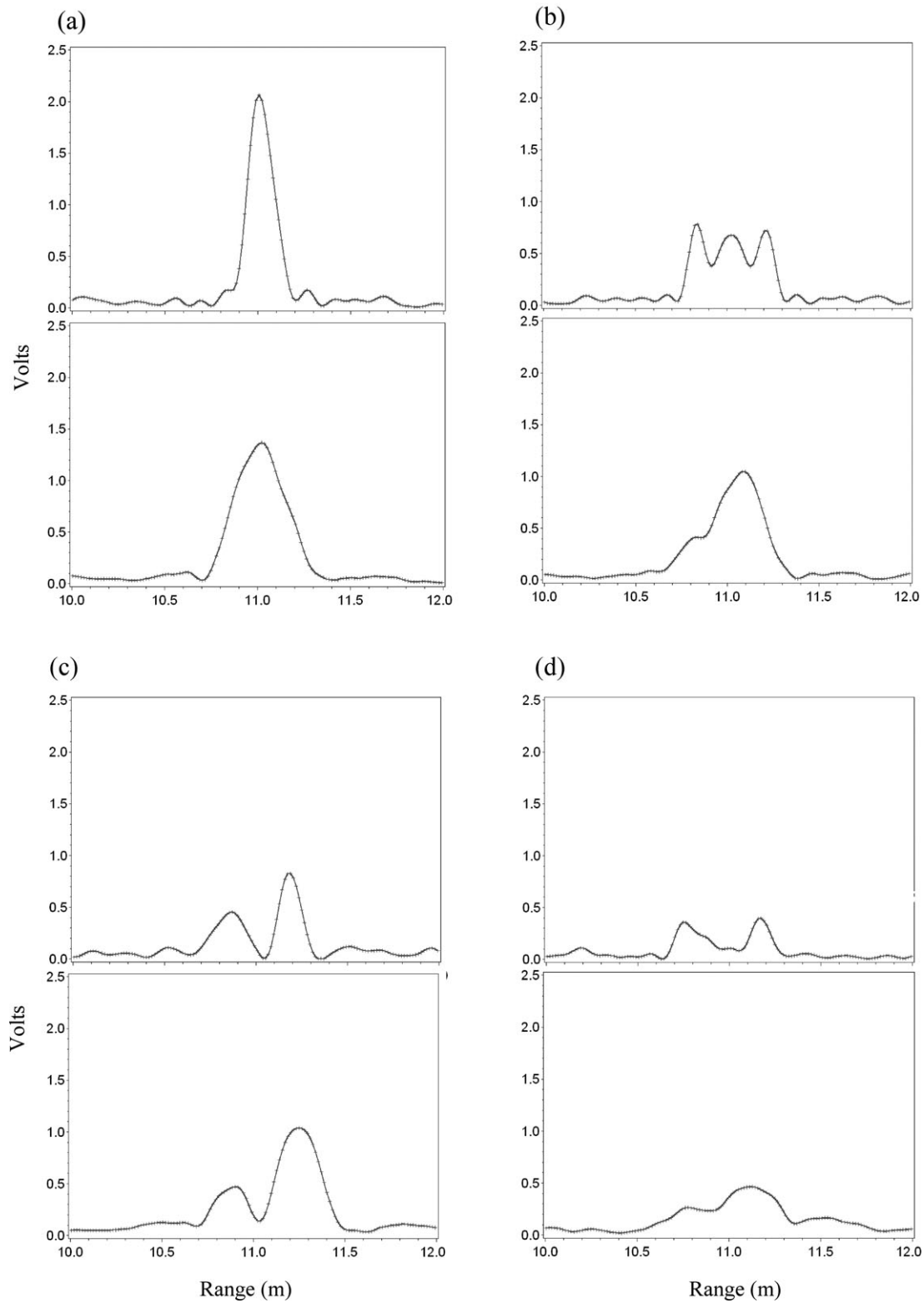


Figure 8. Split-beam echo envelopes from a tethered chinook salmon 108 cm long at four side-aspect angles: (a) 0°, (b) 15°, (c) 20°, and (d) 25°. Each frame compares the envelope shape resulting from a 0.2 ms (top graph) and 0.4 ms (bottom graph) transmit pulse.

data also showed that discrete peaks in echo envelopes often emerged at intervals that exceeded the range resolution of 15 cm, e.g. the three peaks in Figure 6b are each separated by ~ 20 cm.

Our data show that variation in the shape and duration of echoes returned from a fish insonified at side aspect may reflect both the length of the target and the change in orientation. Consequently, in environments where lengths or swimming

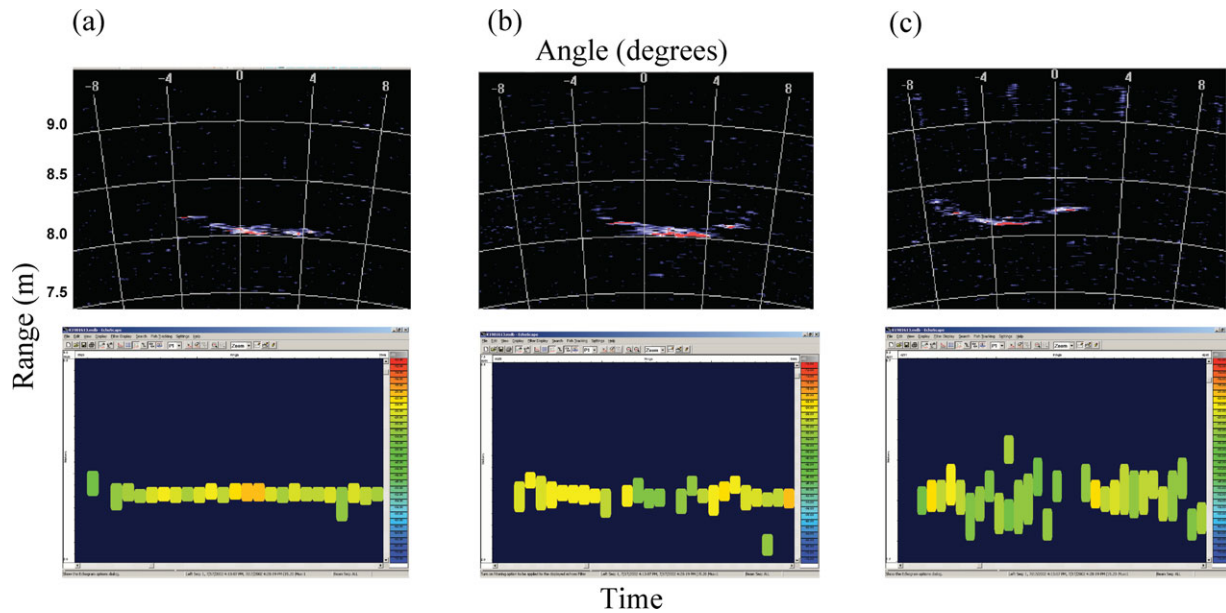


Figure 9. DIDSON images (top) with corresponding split-beam echogram excerpts (bottom) from a tethered chinook salmon 118 cm long showing (a) low activity level (i.e. a low level of undulatory body movement) with the fish body centred on the acoustic axes, (b) high activity level with the fish body centred on the acoustic axes, and (c) high activity level with tail region centred on the acoustic axes. The DIDSON frames show a section of the beam covering 7.5–9 m range and -8 to $+8^\circ$ horizontal angle. The split-beam echograms display 26 sequential echoes from 7.2 to 9 m.

behaviour, or both factors acting together, differ among target species, echo duration measurements may be an effective species discriminator (e.g. Burwen *et al.*, 2003; Fleischman and Burwen, 2003). These results may also have implications for setting single-target acceptance criteria based on echo-envelope widths at defined power points. By setting overly restrictive echo-length filters, potentially useful information from elongated pulses may be lost.

We have presented compelling evidence that high-intensity echoes can be reflected from structures other than gas-filled swimbladders. We acknowledge that these results do not present exhaustive evidence that complex echo shapes come from large fish, but rather that they open the way for controlled experiments that would help illuminate the factors that influence resultant echo shape.

Acknowledgements

This work was supported by the Alaska Department of Fish and Game, the Federal Aid in Sport Fish Restoration Act, the Kenai River Sportfishing Association, the Office of Naval Research (N0014-00-1-0180), the National Ocean Partnership Program (NA050AR4604090), and the Alaska Fisheries Science Center (NA17RJ1232-AM01).

References

Belcher, E. O., Matsuyama, G., and Trimble, R. 2001. Object identification with acoustic lenses. Proceedings of MTS/IEEE Oceans 2001, Honolulu, Hawaii, 1: 6–11.

Burwen, D. L., and Fleischman, S. J. 1998. Evaluation of side-aspect target strength and pulse width as hydroacoustic discriminators of fish species in rivers. Canadian Journal of Fisheries and Aquatic Sciences, 55: 2492–2502.

Burwen, D. L., Fleischman, S. J., and Miller, J. D. Evaluation of a dual-frequency imaging sonar for detecting and estimating the size of

migrating salmon. Fishery Data Series, Alaska Department of Fish and Game, Anchorage, AK, USA (in press).

Burwen, D. L., Fleischman, S. J., Miller, J. D., and Jensen, M. E. 2003. Time-based signal characteristics as predictors of fish size and species for a side-looking hydroacoustic application in a river. ICES Journal of Marine Science, 60: 662–668.

Dahl, P. H., and Mathisen, O. A. 1983. Measurements of fish target strength and associated directivity at high frequencies. Journal of the Acoustical Society of America, 73: 1205–1211.

Dawson, J. J., Wiggins, D., Degan, D., Geiger, H., Hart, D., and Adams, B. 2000. Point-source violations: split-beam tracking of fish at close range. Aquatic Living Resources, 13: 291–295.

Ehrenberg, J. E., and Johnston, S. V. 1996. Evaluation of the use of hydroacoustic pulse width data to separate fish by size group. Report of Hydroacoustic Technology, Inc. to Alaska Department of Fish and Game, Sport Fish Division, Anchorage.

Fleischman, S. J., and Burwen, D. L. 2000. Correcting for position-related bias in estimates of the acoustic backscattering cross-section. Aquatic Living Resources, 13: 283–290.

Fleischman, S. J., and Burwen, D. L. 2003. Mixture models for the species apportionment of hydroacoustic data, with echo envelope length as the discriminatory variable. ICES Journal of Marine Science, 60: 592–598.

Foote, K. G. 1980a. Effect of fish behaviour on echo energy: the need for measurements of orientation distributions. Journal du Conseil International pour L'Exploration de la Mer, 39: 193–201.

Foote, K. G. 1980b. Importance of the swimbladder in acoustic scattering by fish; a comparison of gadoid and mackerel target strengths. Journal of the Acoustical Society of America, 67: 2084–2089.

Harden-Jones, F. R., and Pearce, G. 1950. Acoustic reflection experiments with perch (*Perca fluviatilis* L.) to determine the proportion of echo returned from the swim bladder. Journal of Experimental Biology, 35: 437–450.

Kieser, R., Mulligan, T. K., and Ehrenberg, J. E. 2000. Observation and explanation of systematic split-beam angle measurement errors. Aquatic Living Resources, 13: 275–281.

- Kubecka, J. 1994. Simple model on the relationship between fish acoustical target strength and aspect for high-frequency sonar in shallow waters. *Journal of Applied Ichthyology*, 10: 75–81.
- Lilja, J., Marjomaki, T. J., Jurvelius, J., Rossi, T., and Heikkola, E. 2004. Simulation and experimental measurement of side-aspect target strength of Atlantic salmon (*Salmo salar*) at high frequency. *Canadian Journal of Fisheries and Aquatic Sciences*, 61: 2227–2236.
- Love, R. H. 1969. Maximum side-aspect target strength of an individual fish. *Journal of the Acoustic Society of America*, 46: 746–752.
- MacLennan, D. N., Magurran, A. E., Pitcher, T. J., and Hollingworth, C. E. 1990. Behavioural determinants of fish target strength. *Rapports et Procès-verbaux des Réunions du Conseil International pour l'Exploration de la Mer*, 189: 245–253.
- Miller, J. D., and Burwen, D. L. 2002. Estimates of chinook salmon abundance in the Kenai River using split-beam sonar, 2000. Fishery Data Series No. 02–09. Alaska Department of Fish and Game, Anchorage, AK, USA.
- Mulligan, T. K. 2000. Shallow water fisheries sonar, a personal view. *Aquatic Living Resources* 13: 269–273
- Nash, R. D. M., Sun, Y., and Clay, C. S. 1987. High resolution acoustic structure of fish. *Journal du Conseil International pour L'Exploration de la Mer*, 43: 23–31.
- Sound Metrics Corporation. 2004. Dual-frequency Identification Sonar. DIDSON Operation Manual V4.48. Seattle, WA, 39 pp.
- Stanton, T. K., Reeder, D. B., and Jech, J. M. 2003. Inferring fish orientation from broadband-acoustic echoes. *ICES Journal of Marine Science*, 60: 524–531.
- Sun, Y., Nash, R., and Clay, C. S. 1985. Acoustic measurements of the anatomy of fish at 220 kHz. *Journal of the Acoustical Society of America*, 78: 1772–1776.

doi:10.1093/icesjms/fsm074